Int J Clin Exp Pathol 2019;12(10):3968-3974
www.ijcep.com /ISSN:1936-2625/IJCEP0101935

Original Article

AAVC-I promotes apoptosis of human oral squamous cell carcinoma through the mitochondrial pathway

Lin Chai[1], Tingting Huang[2], Zhenjie Wang[2], Ran Xu[1], Chao Deng[1]

[1]School of Stomatology, [2]Department of Pathophysiology, Wannan Medical College, 22 West Wenchang Road, Wuhu 241002, Anhui Province, China

Received September 5, 2019; Accepted September 24, 2019; Epub October 1, 2019; Published October 15, 2019

Abstract: This study aimed to explore the role and possible mechanism of component I from agkistrodon acutus venom (AAVC-I) in promoting the apoptosis of oral squamous cell carcinoma (OSCC). HN4 cells (a human OSCC cell line) were randomly divided into four experimental groups: low AAVC-I (2.5 μg/mL) group, medium AAVC-I (5 μg/mL) group and high AAVC-I (10 μg/mL) group, as well as control group (AAVC-I, 0 μg/mL). AVVC-I was dissolved in RPMI-1640 medium and added to the culture wells at different concentrations when tumor cells had reached the logarithmic growth phase. After 24 hours, cells were harvested and the inhibitory rate of cell proliferation and the mitochondrial membrane depolarization were measured. Western blotting was used to detect the expression levels of cytochrome c, Bcl-2 associated X protein (Bax), and caspase-3 in the cellular cytoplasm either containing mitochondria or following the removal of mitochondria. Cellular apoptosis was detected by flow cytometry. Compared to the control group, AAVC-I treatment not only inhibited NH4 growth, but also upgraded the expression of caspase-3 in NH4 cells. Meanwhile, it was observed that Bax translocation to mitochondria and cytochrome c release into the cytosol increased in AAVC-I treatment. This indicated that AAVC-I could disrupt mitochondrial membrane depolarization and result in cellular apoptosis, and the apoptosis rate of NH4 increased with the concentration of AAVC-I. The data suggested that AAVC-I promotes the apoptosis of HN4 cells through the mitochondrial pathway in a dose-dependent manner, which provides experimental data and new ideas for future research and clinical treatment options for OSCC.

Keywords: Component I from agkistrodon acutus venom, apoptosis, oral squamous cell carcinoma, mitochondria

Introduction

Oral squamous cell carcinoma (OSCC), also known as oral cancer, is a common malignant tumor in the head and neck, with a high degree of malignancy, accounting for more than 90% of maxillofacial malignancies [1-3]. OSCC is prone to invasion of the nearby glands, muscles and bones, and early lymph node metastasis is the most common. Although current treatments including surgery, radiation therapy and chemotherapy, have been improved dramatically, the mortality of OSCC still remains high [4], and the patient's quality of life and prognosis are not ideal [5, 6]. Moreover, surgery performs to remove tumors often resulting in facial tissue defects, which can bring patients considerable physical and mental traumas [7]. In addition, radiotherapy and chemotherapy can damage normal cells while killing tumor cells, and cause serious complications such as liver and kidney damage, bone marrow suppression, decreased immune function, and even death. Therefore, it is urgent to search for new and effective treatments for OSCC.

Component I from agkistrodon acutus venom (AAVC-I) is a tumor-inhibitory component extracted and purified from the crude venom of the snake D. acutus. It has a remarkable inhibitory effect on tumor cell proliferation and resulting in cellular apoptosis. For example, studies have shown that AAVC-I promotes the apoptosis of lung cancer cells and leukemia cells by regulating the mitochondrial apoptosis pathway [8, 9]. In this study, we investigated the possibility that AAVC-I promotes the apoptosis of OSCC through the mitochondrial apoptosis pathway.

Materials and methods

Preparation of materials

HN4 cells (a human OSCC cell line) were provided by the Department of Oral Medicine of Wannan Medical College. Fetal bovine serum (FBS) was purchased from Zhejiang Tianhang Biotechnology CO., LTD (China). AAVC-I lyophilized powder was provided by the Institute of Snake Venom of Wannan Medical College. Cytochrome c and Bcl-2 associated X protein (Bax) antibodies were purchased from Abcam (USA). COX IV and Cleaved caspase-3 antibodies were purchased from Cell Signaling Technology (USA). The annexin V-FITC apoptosis detection kit, the fluorescent probe JC-1 and MTT assay kit were purchased from Beyotime Institute of Biotechnology (China).

Experimental grouping and administration

Preparation of AAVC-I solution with various concentrations: 0, 2.5, 5.0, and 10.0 μg/mL as control group, low AAVC-I group, medium AAVC-I group and high AAVC-I group respectively.

HN4 cell culture

HN4 cells were resuscitated, and cultured in RPMI-1640 media supplemented with 10% FBS at 37°C, 5% CO_2 in a 95% humidified atmosphere. The cells were passaged normally, and cells in the logarithmic growth phase were harvested for subsequent experiments. All procedures were approved by the Laboratory Committee of Wannan Medical College and conformed to the Guide for the Laboratory of the National Institutes of Health.

Proliferation inhibition rate determination using the MTT assay

According to the scheme described in 2.2, HN4 cells in the logarithmic growth phase were seeded into 96-well plates (n=6) for 24 h. After removal of the supernatant, 20 μL of 1 × MTT solution was added to each well and left to incubate for 4 h. Supernatants were discarded, and 150 μL of DMSO was added to each well and shaken for 10 min. The optical density (OD) values of each well were measured at a wavelength of 570 nm using an enzyme-linked detector. The above experiment was repeated three times. The proliferation inhibition rate (%) was calculated as follows: (1 - OD value of the drug-treatment group/average OD value of the control group) × 100%.

Analysis of mitochondrial membrane depolarization

HN4 cells were exposed for 24 h to AAVC-I at 0, 2.5, 5, and 10 μg/mL respectively. The cells were stained with a JC-1 probe to measure mitochondrial membrane depolarization, according to the manufacturer's instructions. The cells were incubated with an equal volume of JC-1-staining solution at 37°C for 30 min and washed with phosphate buffered saline (PBS) (Boster, Wuhan, China). The mitochondrial membrane potentials were monitored by determining the relative amounts of dual emissions from both mitochondrial JC-1 monomers and aggregates using a fluorescence microscope (Nikon, Japan). The rate of aggregated JC-1 and monomeric JC-1 represented mitochondrial membrane depolarization of HN4 cells.

Western blotting

Cells were harvested after 24 h of AAVC-I treatment. Proteins were extracted according to the instructions of the mitochondrial tissue isolation kit [10]. The cell pellet was gently resuspended in ice-cold PBS, and a small number of cells were used for counting. The remaining cells were centrifuged at 600 × *g* until pelleted, followed by discarding of the supernatants. Cells were then homogenized on ice, and centrifuged at 1,000 × *g* for 10 min at 4°C to pellet the cells. The supernatants were discarded, followed by centrifugation at 3,500 × *g* for 10 min at 4°C. The resulting pellet was then used for mitochondrial isolation. The supernatants were centrifuged at 12,000 × *g* for 10 min at 4°C, and the resulting supernatants were mitochondria-free cytoplasmic proteins. HN4 cells were homogenized, and centrifuged at 12,000 × *g* for 15 min at 4°C. The protein content of each sample was determined using a protein assay kit (Abcam, American). The extracted proteins were separated by 15% SDS-PAGE, followed by transfer to a PVDF membrane. The membrane was blocked with 5% skim milk for 1 h, and then incubated with the primary antibodies and an internal reference overnight. The following day, the membrane was rinsed with Tris-Buffered Saline Tween (TBST) three times for 10 min each. The membrane was then incubated with

A **Effect of AAVC-I on the growth of HN4 cells**

Group	OD	Inhibition rate (%)
Control	1.04±0.06	-
AAVC-I (2.5 μg/mL)	0.88±0.04*	14.89±1.48*
AAVC-I (5 μg/mL)	0.79±0.05*[a]	23.71±2.62*[a]
AAVC-I (10 μg/mL)	0.53±0.05**[b]	48.86±3.85**[b]

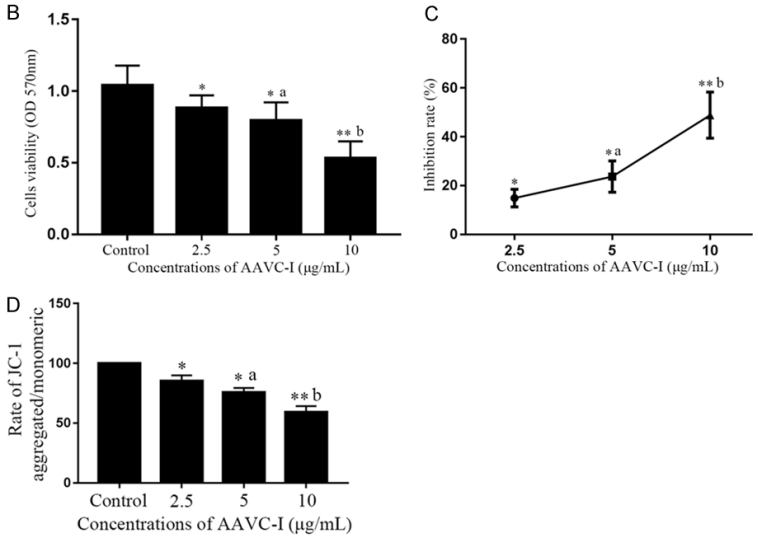

Figure 1. The proliferation of HN4 cells *in vitro* was inhibited after treatment by AAVC-I (A-C). Effect of AAVC-I on mitochondrial membrane potential in HN4 cells. Mitochondrial membrane potential was measured using JC-1 assay kit (D). The data shown in the graph represent the mean ± SD deviation of triplicate experiments (n=6). **P<0.01, *P<0.05 vs. control group; [a]P>0.05 vs. low AAVC-I group (2.5 μg/mL); [b]P<0.05 vs. medium AAVC-I group (5 μg/mL).

horseradish peroxidase (HRP)-labeled secondary antibodies for 2 h, and rinsed three times with TBST for 10 min. An ECL luminescence kit was then used to reveal the bands. Protein levels were analyzed using UN-SCAN-IT software (Silk Scientific Inc., Orem, UT, USA).

Apoptosis detection by flow cytometry

After 24 h of treatment with AAVC-I, cells were harvested and digested with EDTA-free trypsin and then centrifuged. The cells were collected and washed with pre-cooled PBS, followed by centrifugation at 1,000 × *g* for 5 min. After removal of the supernatants, the cells were gently resuspended in 400 μL of annexin V binding solution, followed by cell counting. 5 μL of annexin V-FITC was added, gently mixed, and left to incubate for 15 min at 2-8°C. 10 μL of propidium iodide staining solution was added, mixed, and incubated for 5 min at 2-8°C, followed immediately by detection with flow cytometry. The experiment was repeated three times.

Statistical analysis

SPSS 18.0 software was used for data processing and statistical analysis. All data are expressed as the mean ± standard deviation (X ± SD). An ANOVA was used for multiple group comparisons. P<0.05 was considered a significant difference.

Results

Effects of AAVC-I on HN4 cells proliferation and mitochondrial membrane depolarization

The effect of AAVC-I on the proliferation of HN4 oral cancer cells was determined using an MTT assay. Results showed that AAVC-I significantly inhibited the proliferation of HN4 cells *in vitro*, in a concentration-dependent manner (**Figure 1A-C**). As for the JC-1 staining, JC-1 aggregates (red fluorescence) were prominent in the control group. Exposure of HN4 cells to AAVC-I resulted in decrease of red fluorescence and increase of green fluorescence, indicating a loss in mitochondrial membrane potential (**Figure 1D**).

Expression of cytochrome c and Bax in the mitochondria and cytoplasm of HN4 cells after AAVC-I treatment

After 24 h of AAVC-I treatment, cells were harvested, and the expression of cytochrome c and Bax in the mitochondria and cytoplasm of HN4 cells was detected by western blotting. Results showed that following treatment with AAVC-I, cytochrome c in the mitochondrial fraction and Bax in the cytoplasmic fraction were decreased, whereas cytochrome c in the cytoplasmic fraction and Bax in the mitochondrial fraction were increased. The effect was also AAVC-I concentration-dependent (**Figure 2**).

Expression of caspase-3 in HN4 cells after AAVC-I treatment

It has been reported that caspase-3 activation leads to the cleavage of various proteins, ulti-

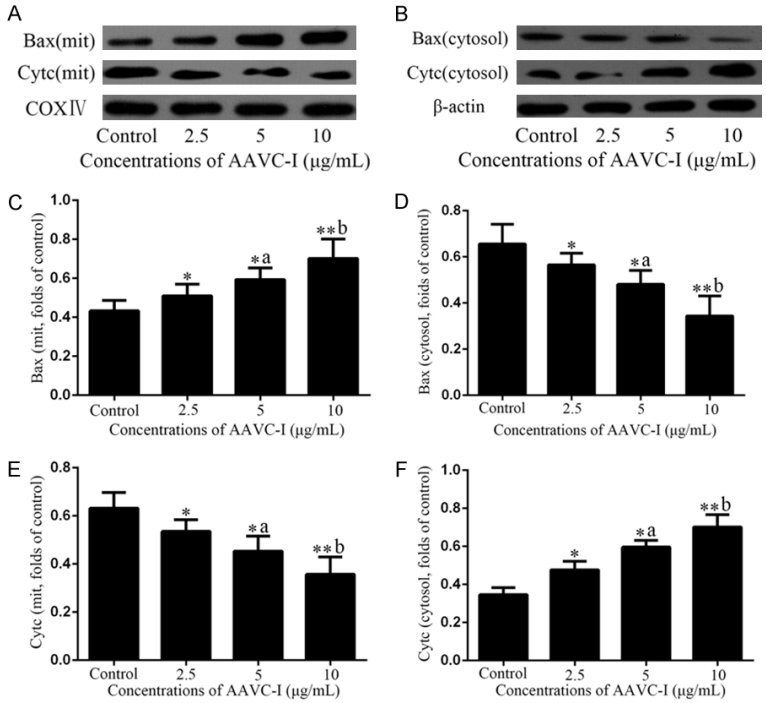

Figure 2. Effect of AAVC-I on pro-apoptotic protein expression of HN4 cells. (A, B) The expression of Bax and cytochrome c in the ipsilateral cortex was evaluated by western blotting 24 h after AAVC-I treatment. Representative blots show the relative expression of (C, E) mitochondrial and (D, F) cytosolic Bax and cytochrome c. Expression was normalized to the level of COX IV or β-actin. Data represent the mean ± SD (n=6). $^{**}P<0.01$, $^{*}P<0.05$ vs. control group; $^{a}P<0.05$ vs. low AAVC-I group (2.5 μg/mL); $^{b}P<0.05$ vs. medium AAVC-I group (5 μg/mL).

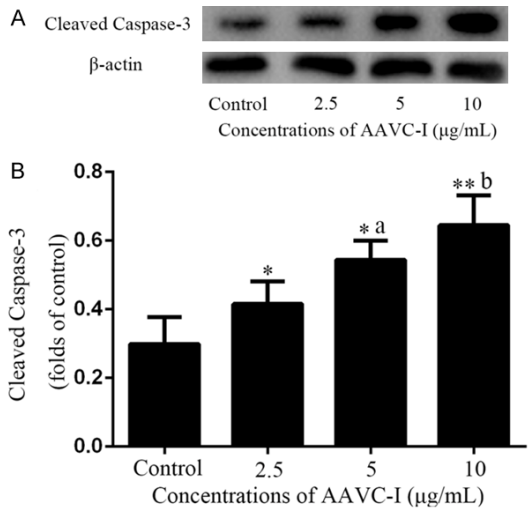

Figure 3. Effect of AAVC-I on caspase-3 expression in HN4 cells. Experimental groups are as defined in the **Figure 4** legend. Caspase-3 expression was assessed 24 h after AAVC-I treatment, using western blot. Data represent the mean ± SD (n=6). $^{**}P<0.01$, $^{*}P<0.05$ vs. control group; $^{a}P<0.05$ vs. low AAVC-I group (2.5 μg/mL); $^{b}P<0.05$ vs. medium AAVC-I group (5 μg/mL).

mately resulting in DNA fragmentation and apoptosis [11]. In this study, after 24 h of treatment with AAVC-I, cells were harvested and the expression of caspase-3 was detected by western blotting. Results showed that treatment with increasing concentrations of AAVC-I resulted in concomitant increases in the expression levels of caspase-3, indicating that AAVC-I enhanced apoptosis and the apoptosis rate was dose-dependent (**Figure 3**).

Apoptosis of HN4 cells after AAVC-I treatment

Flow cytometry was used to detect the apoptosis of HN4 cells. Compared with the control group, the apoptosis rate of HN4 cells treated with AAVC-I was increased. The apoptosis rate of the high dose group was higher than that of low dose group, which indicated that AAVC-I could significantly induce the apoptosis of HN4 cells in a dose-dependent manner (**Figure 4**).

Discussion

Oral cancer is acommon malignant tumor, and it can seriously decrease the quality of life and mental health of afflicted patients. There are approximately 100,000 newly-diagnosed cases worldwide every year [12]. The current available treatments focus on relieving of symptoms and delaying progression of the disease. It is reported that the 5-year survival rate of patients with advanced forms of the disease is still low [13-15].

Chemotherapy is one of the main treatments for oral cancer, thus developing new and effective anti-tumor drugs is an intense area of study. Snake venom has broad application prospects in anti-tumor treatment. A variety of anti-tumor components have been extracted from crude snake venom, such as metalloproteinases (MPs), L-amino acid oxidases (LAAOs) and

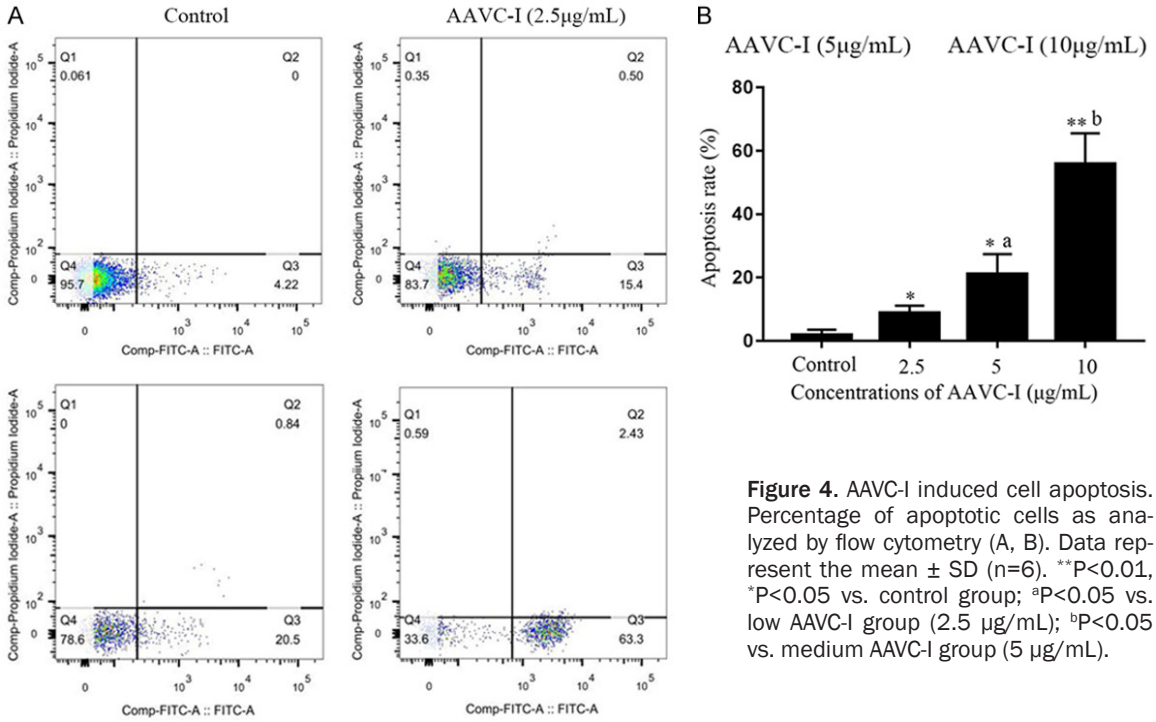

Figure 4. AAVC-I induced cell apoptosis. Percentage of apoptotic cells as analyzed by flow cytometry (A, B). Data represent the mean ± SD (n=6). $^{**}P<0.01$, $^{*}P<0.05$ vs. control group; $^{a}P<0.05$ vs. low AAVC-I group (2.5 μg/mL); $^{b}P<0.05$ vs. medium AAVC-I group (5 μg/mL).

C-type lectin. These components have exerted their anti-tumor functions through different pathways [16]. ACTX-8, a cytotoxic L-amino acid oxidase isolated from Agkistrodon acutus snake venom, induces apoptosis in Hela cervical cancer cells [17].

AAVC-I, a component extracted from the venom of the snake D. acutus, induces apoptosis [18]. However, the potential mechanism underlying this phenomenon is still unknown. This study aimed to explore the effect and possible mechanisms of AAVC-I in inducing apoptosis of human HN4 oral cancer cells.

Apoptosis, that is, the process of programmed cell death, is regulated by certain genes, which are critical for cellular differentiation, tissue and organ formation, as well as homeostasis [19]. It has been shown that a variety of anti-tumor chemotherapeutics act by promoting apoptosis [20]. Mitochondria can regulate the cell's membrane potential, and play a role in controlling apoptosis [21]. Under certain stimuli, permeability transition channels can be formed at contact sites between the inner mitochondrial membrane and the outer membrane, leading to increased permeability of the mitochondrial membrane. This induces an irreversible decline in mitochondrial transmembrane potential, eventually resulting in apoptosis. Increased mitochondrial membrane permeability also enables the release of apoptosis inducing factor (AIF), as well as other molecules, into the cytoplasmic matrix to affect cell structure. Bcl-2 is an apoptosis-inhibitory gene, whereas Bax, a member of the Bcl-2 family, can promote apoptosis [22]. Bax has pore-forming abilities which lead to the release of cytochrome c from mitochondria into the cytoplasm [23, 24]. In the presence of dATP, Bax binds to apoptotic protease activating factor-1 (Apaf-1) to activate caspase-9, which subsequently activates caspase-3, to initiate apoptosis [25, 26]. AIF enhances apoptotic signaling by promoting the release of cytochrome c from mitochondria and rapidly activating endonucleases. Our study demonstrated that following treatment with AAVC-I, Bax protein content increased in the mitochondria and decreased in the cytoplasm, suggesting that AAVC-I may lead to the formation of Bax-dependent pore complexes on mitochondria. On the other hand, AAVC-I treatment led to a decrease in cytochrome c in mitochondria, and an increase in the cytoplasm, indicating a release of cytochrome c from the mitochondria to the cytoplasm in HN4 cells. Our results of caspase-3 detection and the inhibition of HN4 cell proliferation following AAVC-I treatment were also in line with our hypothesis that AAVC-I promotes apoptosis.

Conclusion

AAVC-I inhibited HN4 cell proliferation and promoted apoptosis. A possible mechanism was that AAVC-I induced HN4 apoptosis through the mitochondrial pathway. This provides a theoretical basis for the clinical application of AAVC-I, although the effectiveness of AAVC-I in the treatment of oral cancer still requires further study.

Acknowledgements

This work was supported by grants from the Anhui key Projects of Natural Science Research in Colleges and Universities (KJ2017A255), Cultivation Fund for key Scientific Research Projects of Wannan Medical College for 2015 (WK2015Z08), Wuhu Science and Technology Plan Project for 2015 (2015cxy11), Research Project Fund for College Students of Wannan Medical College for 2019 (WK2019S24).

Disclosure of conflict of interest

None.

Abbreviations

AAVC-I, component I from agkistrodon acutus venom; OSCC, oral squamous cell carcinoma; Bax, Bcl-2 associated X protein; OD, optical density; MPs, metalloproteinases; LAAOs, L-amino acid oxidases; AIF, apoptosis inducing factor; Apaf-1, apoptotic protease activating factor-1.

Address correspondence to: Chao Deng, School of Stomatology, Wannan Medical College, 22 West Wenchang Road, Wuhu 241002, Anhui Province, China. Tel: +86-553 3932065; Fax: +86-553 393-2065; E-mail: 20120015@wnmc.edu.cn

References

[1] Sritippho T, Chotjumlong P and Iamaroon A. Roles of human papillomaviruses and p16 in oral cancer. Asian Pac J Cancer Prev 2015; 16: 6193-6200.

[2] Iamaroon A, Pattanaporn K, Pongsiriwet S, Wanachantararak S, Prapayasatok S, Jittidecharaks S, Chitapanarux I and Lorvidhaya V. Analysis of 587 cases of oral squamous cell carcinoma in Northern Thailand with a focus on young people. Int J Oral Maxillofac Surg 2004; 33: 84-88.

[3] Vargas-Ferreira F, Nedel F, Etges A, Gomes AP, Furuse C and Tarquinio SB. Tarquinio, etiologic factors associated with oral squamous cell carcinoma in non-smokers and non-alcoholic drinkers: a brief approach. Braz Dent J 2012; 23: 586-590.

[4] Krisanaprakornkit S and Iamaroon A. Epithelial-mesenchymal transition in oral squamous cell carcinoma. ISRN Oncol 2012; 2012: 681469.

[5] Bauer K, Dowejko A, Bosserhoff AK, Reichert TE and Bauer RJ. P-cadherin induces an epithelial-like phenotype in oral squamous cell carcinoma by GSK-3beta-mediated Snail phosphorylation. Carcinogenesis 2009; 30: 1781-1788.

[6] Bufalino A, Cervigne NK, de Oliveira CE, Fonseca FP, Rodrigues PC, Macedo CC, Sobral LM, Miguel MC, Lopes MA, Paes Leme AF, Lambert DW, Salo TA, Kowalski LP, Graner E and Coletta RD. Low miR-143/miR-145 cluster levels induce activin A overexpression in oral squamous cell carcinomas, which contributes to poor prognosis. PLoS One 2015; 10: e0136599.

[7] Zhu GC, Yu CY, She L, Tan HL, Li G, Ren SL, Su ZW, Wei M, Huang DH, Tian YQ, Su RN, Liu Y and Zhang X. Metadherin regulation of vascular endothelial growth factor expression is dependent upon the PI3K/Akt pathway in squamous cell carcinoma of the head and neck. Medicine (Baltimore) 2015; 94: e502.

[8] Xu P, Zhang GB, Wang F, Wu J, Huang FZ. Inhibitory effect of anti-tumor component I from Agkistrodon acutus venom on human lung cancer A549 cells (in Chinese). Chin Clin Pharmacol Ther 2014; 19: 493-496.

[9] Zheng RQ, Zhang GB, Huang L, Ma KR, Wu J and Li S. Mitochondrial mechanisms of apoptosis of human leukemia K562 cells induced by AAVC-I. Zhongguo Shi Yan Xue Ye Xue Za Zhi 2013; 21: 591-595.

[10] Wei W, Wang H, Wu Y, Ding K, Li T, Cong Z, Xu J, Zhou M, Huang L, Ding H and Wu H. Alpha lipoic acid inhibits neural apoptosis via a mitochondrial pathway in rats following traumatic brain injury. Neurochem Int 2015; 87: 85-91.

[11] Slee EA, Harte MT, Kluck RM, Wolf BB, Casiano CA, Newmeyer DD, Wang HG, Reed JC, Nicholson DW, Alnemri ES, Green DR and Martin SJ. Ordering the cytochrome c-initiated caspase cascade: hierarchical activation of caspases-2, -3, -6, -7, -8, and -10 in a caspase-9-dependent manner. J Cell Biol 1999; 144: 281-292.

[12] Bose P, Brockton NT and Dort JC. Head and neck cancer: from anatomy to biology. Int J Cancer 2013; 133: 2013-2023.

[13] Su SC, Lin CW, Liu YF, Fan WL, Chen MK, Yu CP, Yang WE, Su CW, Chuang CY, Li WH, Chung WH and Yang SF. Exome sequencing of oral squamous cell carcinoma reveals molecular subgroups and novel therapeutic opportunities. Theranostics 2017; 7: 1088-1099.
[14] Ikebe T, Takeuchi H, Jimi E, Beppu M, Shinohara M and Shirasuna K. Involvement of proteasomes in migration and matrix metalloproteinase-9 production of oral squamous cell carcinoma. Int J Cancer 1998; 77: 578-585.
[15] Wu JY, Yi C, Chung HR, Wang DJ, Chang WC, Lee SY, Lin CT, Yang YC and Yang WC. Potential biomarkers in saliva for oral squamous cell carcinoma. Oral Oncol 2010; 46: 226-231.
[16] Calderon LA, Sobrinho JC, Zaqueo KD, de Moura AA, Grabner AN, Mazzi MV, Marcussi S, Nomizo A, Fernandes CF, Zuliani JP, Carvalho BM, da Silva SL, Stábeli RG and Soares AM. Antitumoral activity of snake venom proteins: new trends in cancer therapy. Biomed Res Int 2014; 2014: 203639.
[17] Zhang L and Wei LJ. ACTX-8, a cytotoxic L-amino acid oxidase isolated from Agkistrodon acutus snake venom, induces apoptosis in Hela cervical cancer cells. Life Sci 2007; 80: 1189-97.
[18] Zhou B, Zhang GB, Duan T, Zhou J and Wu J. Component I from Agkistrodon acutus venom induces apoptosis of K562/A02 cells by promoting caspase 3 expression. Zhongguo Shi Yan Xue Ye Xue Za Zhi 2012; 20: 273-6.
[19] Goldar S, Khaniani MS, Derakhshan SM and Baradaran B. Molecular mechanisms of apoptosis and roles in cancer development and treatment. Asian Pac J Cancer Prev 2015; 16: 2129-44.
[20] Opzoomer JW, Sosnowska D, Anstee JE, Spicer JF and Arnold JN. Cytotoxic chemotherapy as an immune stimulus: a molecular perspective on turning up the immunological heat on cancer. Front Immunol 2019; 10: 1654.
[21] Galluzzi L, Morselli E, Kepp O and Kroemer G. Targeting post-mitochondrial effectors of apoptosis for neuroprotection. Biochim Biophys Acta 2009; 1787: 402-413.
[22] Yin XM. Signal transduction mediated by bid, a pro-death Bcl-2 family proteins, connects the death receptor and mitochondria apoptosis pathways. Cell Res 2000; 10: 161-167.
[23] Deng C, Sun Z, Tong G, Yi W, Ma L, Zhao B, Cheng L, Zhang J, Cao F and Yi D. Alpha-lipoic acid reduces infarct size and preserves cardiac function in rat myocardial ischemia/reperfusion injury through activation of PI3K/Akt/Nrf2 pathway. PLoS One 2013; 8: e58371.
[24] Xiao S, Chen F and Gao C. Antitumor activity of 4-O-methylhonokiol in human oral cancer cells is mediated via ROS generation, disruption of mitochondrial potential, cell cycle arrest and modulation of Bcl-2/Bax proteins. J BUON 2017; 22: 1577-1581.
[25] Dai F, Gao L, Zhao Y, Wang C and Xie S. Farrerol inhibited angiogenesis through Akt/mTOR, Erk and Jak2/Stat3 signal pathway. Phytomedicine 2016; 23: 686-693.
[26] Seo JH, Choi HW, Oh HN, Lee MH, Kim E, Yoon G, Cho SS, Park SM, Cho YS, Chae JI and Shim JH. Licochalcone D directly targets JAK2 to induced apoptosis in human oral squamous cell carcinoma. J Cell Physiol 2019; 234: 1780-1793.